Acta Radiologica Open
4(2) 1–9
© The Foundation Acta Radiologica 2015
Reprints and permissions:
sagepub.co.uk/journalsPermissions.nav
DOI: 10.1177/2047981614561285
arr.sagepub.com

Comparison of gadoxetic acid and gadopentetate dimeglumine-enhanced MRI for HCC detection: prospective crossover study at 3 T

Cecilia Besa[1,2], Suguru Kakite[2], Nancy Cooper[1], Marcelo Facciuto[3] and Bachir Taouli[1,2]

Abstract

Background: Gadoxetic acid and gadopentetate dimeglumine are gadolinium-based contrast agents (GBCAs) with an established role in HCC detection and characterization.

Purpose: To compare gadopentetate dimeglumine and gadoxetic acid-enhanced magnetic resonance imaging (MRI) for image quality and hepatocellular carcinoma (HCC) detection/conspicuity.

Material and Methods: In this IRB approved cross-over pilot prospective study, 12 patients (all men; mean age, 56 years) with chronic liver disease at risk of HCC underwent two repeat MRI examinations using gadopentetate dimeglumine and gadoxetic acid (mean interval between studies, 5 days). Two independent observers analyzed images for image quality and HCC detection/conspicuity. Per-lesion sensitivity, positive predictive value, quantitative enhancement, and lesion-to-liver contrast ratio were calculated for both contrast agents.

Results: There was no significant difference in image quality scores between both GBCAs ($P = 0.3$). A total of 20 HCCs were identified with reference standard in 12 patients (mean size 2.6 cm, range, 1.0–5.0 cm). Higher sensitivity was seen for observer 1 for gadoxetic acid-set in comparison with gadopentetate dimeglumine-set (sensitivity increased from 85.7% to 92.8%), while no difference was noted for observer 2 (sensitivity of 78.5%). Lesion conspicuity was significantly higher on hepatobiliary phase (HBP) images compared to arterial phase images with both GBCAs for both observers ($P < 0.05$). Lesion-to-liver contrast ratios were significantly higher for HBP compared to all dynamic phases for both agents ($P < 0.05$).

Conclusion: Our initial experience suggests that gadoxetic acid-set was superior to gadopentetate dimeglumine-set in terms of HCC detection for one observer, with improved lesion conspicuity and liver-to-lesion contrast on HBP images.

Keywords
Liver, hepatocarcinoma, magnetic resonance imaging, Gd-EOB-DTPA, Gd-DTPA

Date received: 5 September 2014; accepted: 31 October 2014

Introduction

Hepatocellular carcinoma (HCC) is the most common primary hepatic malignancy, and usually develops in the setting of liver cirrhosis. Over the last 20 years, the incidence of HCC in the US has increased from 1.5 to 4.9 per 100,000; with a concomitant 41% increase in overall mortality rate (1). Therefore, accurate detection and identification of the number, size, and location of HCC is critical for staging and treatment planning. However, in practice this can be challenging due to the

[1]Department of Radiology, Body MRI, Icahn School of Medicine at Mount Sinai, New York, NY, USA
[2]Translational and Molecular Imaging Institute, Icahn School of Medicine at Mount Sinai, New York, NY, USA
[3]Recanati/Miller Transplantation Institute, Icahn School of Medicine at Mount Sinai, New York, NY, USA

Corresponding author:
Bachir Taouli, Icahn School of Medicine at Mount Sinai, Translational and molecular Imaging Institute, One Gustave Levy Place, New York, NY 10029, USA.
Email: bachir.taouli@mountsinai.org

Creative Commons CC-BY-NC: This article is distributed under the terms of the Creative Commons Attribution-NonCommercial 3.0 License (http://www.creativecommons.org/licenses/by-nc/3.0/) which permits non-commercial use, reproduction and distribution of the work without further permission provided the original work is attributed as specified on the SAGE and Open Access page (http://www.uk.sagepub.com/aboutus/openaccess.htm).

imaging variability of HCCs and the possibility of encountering benign lesions in cirrhotic liver.

Contrast-enhanced magnetic resonance imaging (CE MRI) using extracellular gadolinium-based contrast agents (GBCAs) has proven an excellent imaging technique to detect and stage HCC (2,3). Gadolinium ethoxybenzyl diethylenetriamine pentaacetic acid (Gd-EOB-DTPA or gadoxetic acid, Eovist/Primovist) is a liver-specific GBCA derivative of Gd-DTPA that produces both dynamic and liver specific hepatobiliary images, allowing for lesion detection and characterization (4–10). This contrast agent is highly liver-specific, with approximately 50% of the injected dose taken up by functioning hepatocytes and excreted in bile (11). Recent published data have shown high accuracy of gadoxetic acid for HCC detection (12–14). There are few prior studies comparing extracellular GBCAs to gadoxetic acid in terms of liver lesion detection; these have shown improved lesion conspicuity during hepatobiliary phase (HBP) after administration of gadoxetic acid due to increased contrast between liver parenchyma and focal liver lesions including HCC (4,15). Two studies from South Korea have specifically addressed HCC detection (16,17). Park et al. (16) in a study of 43 patients with 59 HCCs retrospectively compared gadoxetic acid to gadopentetate dimeglumine for HCC detection (up to 2 cm in size) using a 1.5 T system, and showed no significant differences in the diagnostic accuracy for HCC detection, with however significantly higher sensitivity for gadoxetic acid (86.4%) compared to gadopentetate dimeglumine (64.4%) due to better delineation of HCC on HBP imaging. The other study (17) compared gadoxetic acid to gadobenate dimeglumine (Gd-BOPTA) in 18 patients with 22 HCCs imaged at 3 T, and found equivalent sensitivity for both agents: 80–83% for gadoxetic acid vs. gadobenate dimeglumine, respectively.

The aims of this prospective pilot cross-over study were to compare 3D contrast-enhanced T1-weighted (T1W) images obtained at 3 T using both gadopentetate dimeglumine and gadoxetic acid in patients with chronic liver disease and HCC in terms of:

- Image quality and degree of enhancement of HCC, liver parenchyma, and hepatic vessels;
- HCC detection and conspicuity.

Material and Methods

Patients

This was an IRB approved prospective crossover single center study funded by Bayer Healthcare comparing gadopentetate dimeglumine (Magnevist, Bayer Schering Pharma, Berlin, Germany) to gadoxetic acid (Eovist/Primovist, Schering Pharma, Berlin, Germany). Twelve patients (all men; mean age, 56 ± 8.7 years, age range, 42–71 years; weight, 76 kg; range 57–137 kg) with chronic liver disease secondary to HCV ($n = 9$), alcohol ($n = 2$), HBV ($n = 1$), and NASH ($n = 1$) and suspected of having HCC based on prior computed tomography (CT) were enrolled prospectively in the study, and underwent two repeat MR examinations with both GBCAs with a mean interval of 5 days (range, 1–15 days) between November 2010 and November 2012. All study participants provided signed informed consent prior to entry into the study. Eleven out of 12 patients (90%) had liver cirrhosis on imaging that was pathologically confirmed in seven cases. One patient was non-cirrhotic. Seven of 12 patients received locoregional therapy for HCC using transarterial chemoembolization (TACE) and/or radiofrequency embolization (RFA) and one segmental Y90 radioembolization before being enrolled in the study. Three of 12 patients were enrolled before undergoing liver transplantation and received locoregional treatment as a bridge therapy before transplant. Bilirubin levels were 1.2 mg/dl (range, 0.5–2.5 mg/dl).

MRI

All patients received two GBCAs (gadopentetate dimeglumine and gadoxetic acid) with dynamic imaging and hepatobiliary phase (HBP) imaging for gadoxetic acid on two separate days. As part of the research protocol, all the patients received first gadopentetate dimeglumine followed by gadoxetic acid. All patients underwent a liver MRI protocol using a state-of-the-art multichannel 3 T system (GE 750, GE Healthcare, Waukesha WI, USA) equipped with a 32-channel phased-array coil. The protocol included the following sequences (all sequences were breath-hold with Array Spatial Sensitivity Encoding Technique (ASSET) 2, except for diffusion-weighted imaging (DWI) which was acquired in free breathing: coronal single shot fast spin echo (SSFSE) T2, axial SSFSE with long TE, axial fat suppressed (FS) T2 fast spin echo (FSE), axial DWI and pre/post-contrast dynamic axial 3D T1 Liver acquisition with volume acceleration (LAVA) FLEX sequence with in- and out-of-phase and HBP images for gadoxetic acid (Table 1). During the repeat exam, only the following sequences were acquired: DWI and pre-/postcontrast T1 LAVA.

LAVA contrast-enhanced T1W 3D GRE technique enables whole liver coverage with high speed and spatial resolution during a single breath hold. In this study, we used a LAVA FLEX sequence, which allows acquisition, in one scan, of four different contrasts, with output images including in-phase, opposed-phase,

Table 1. MR sequence parameters used for the study.

	Coronal T2WI SSFSE	Axial T2WI SSFSE	FS FSE T2WI	DWI*	LAVA FLEX T1WI
TR	969.2–2812.9	1219–2268.6	2000–2400	2000–6000	3.948–4.892
TE	97–102.5	177.6–240.2	96.1–103.6	55.4–57.2	1.716–2.056
FA	90	90	90	90	10
Matrix	320*256	320*256	256*256	128*128	512*512 (ZIP)
FOV	340–430	340–430	340–430	340–430	320–430
Slice (mm)	5	4	7	7	4–5.6
Interval (mm)	1	1	1	1.6	0
Parallel imaging	2	2	2	2	2x2

*DWI: b values 0, 50, 500, 1000.

FA, flip angle; DWI, diffusion-weighted imaging; FOV, field of view; FS FSE, fat suppressed fast spin echo; LAVA, liver acquisition with volume acquisition; SSFSE, single shot fast spin echo; T1WI: T1-weighted imaging; T2WI, T2-weighted imaging; TE, echo time; TR, repetition time.

water and fat images. After the acquisition of precontrast sequences, the following GBCAs were injected on two different sessions: gadopentetate dimeglumine at a dose of 0.1 mmol/kg, and a fixed dose of 10 mL of gadoxetic acid (corresponding to a mean weight-based dose of 0.03 mmol/kg, in the range of 0.0183–0.04 mmol/kg). The fixed dose of gadoxetic acid corresponds to our current standard of care clinical practice. GBCAs were injected at a rate of 2 mL/s (for gadopentetate dimeglumine) and 1.5 mL/s (for gadoxetic acid) via a power injector followed by a 20 mL saline flush, with images acquired at early arterial (AP1 at approximately 20 s), late arterial (AP2 at approximately 30 s) (two sequences back-to-back in one breath-hold), followed by portal venous phase (PVP, at 60 s), and late venous phase (LVP, at 180 s). AP1 images were acquired using a bolus tracking technique for both agents. Hepatobiliary phase (HBP) images were obtained 10 and 20 min after gadoxetic acid injection in the axial and coronal planes.

Image evaluation

Two observers (observer 1 and observer 2, with 1 and 3 years of abdominal MRI experience) who were blinded to the clinical information and pathological results analyzed independently the MR images in two different sessions (gadoxetic acid-set vs. gadopentetate dimeglumine-set), separated by at least 6 weeks to avoid recall bias. Gadoxetic acid and gadopentetate dimeglumine CE MRI including; 3D T1W LAVA FLEX precontrast, early and late arterial, portal venous and late venous phases with subtraction images were available for the two datasets. In addition, observers had access to precontrast sequences (T2WI, DWI, and T1 in- and opposed-phase) for both sets of CE MRI to allow differentiating HCC from benign lesions such as liver hemangiomas among others.

Image quality and vascular enhancement. The two observers determined the overall image quality using the following subjective scale: 1, poor image quality with major artifacts; 2, acceptable image quality with some artifacts; 3, good image quality, with minimal artifacts; and 4, excellent image quality, no artifacts. They also analyzed the degree of vascular enhancement (aorta/hepatic artery, portal vein [PV], and hepatic veins [HV]) on LAVA FLEX T1WI for each dynamic postcontrast phase (AP1, AP2, PVP, LVP) using the following scale: 0, no appreciable vascular enhancement; 1, poor vascular enhancement; 2, moderate vascular enhancement; 3, good vascular enhancement; and 4, excellent vascular enhancement.

HCC detection/conspicuity. The observers were asked to detect HCCs with a diameter $\geq$1 cm and provide segmental location on hard copies of diagrams of liver anatomy (with Couinaud segments delineated) with corresponding slice number and lesion size. A maximum number of seven HCCs per patient was recorded. Viable HCCs were diagnosed on dynamic MRI according to the American Association for Study of Liver Diseases (AASLD) 2011 criteria (18) when a nodule showed wash-in followed by wash-out and/or capsule/pseudocapsule on PVP and/or LVP. In addition, atypical enhancing lesions with wash-in and no wash-out or hypovascularity were diagnosed as HCC on gadoxetic acid MRI when they showed hypointensity on HBP and hyperintensity on high b value DWI with corresponding hypointensity on apparent diffusion coefficient (ADC) map (3,12). Complete necrotic HCCs post locoregional therapy was diagnosed when a lesion showed absence of contrast enhancement on CE T1W imaging using image subtraction (19), these lesions were excluded from the analysis.

HCC lesion conspicuity of detected lesions was also assessed for each postcontrast phase using the

following scores: 0, not seen; 1: barely conspicuous; 2: fairly well seen; 3: moderately well seen; 4: well seen; and 5: very well seen.

Quantitative analysis of HCC and hepatic enhancement. Two additional observers (observer 3 and observer 4, with 3 and 10 year experience in body MRI) reviewed all the images for the two datasets and identified HCC lesions with a diameter $\geq$1.0 cm in consensus (see below in reference standard). Observer 3 placed regions of interest (ROIs) on HCCs, liver parenchyma, and major hepatic vessels (abdominal aorta used as a surrogate for the hepatic artery, extrahepatic portal vein, and largest hepatic vein) to measure SI on precontrast imaging and on all dynamic imaging phases (AP1, AP2, PVP, LVP) and HBP at 20 min after contrast injection, for all patients. Osirix software (ver 4.1.2, Pixmeo) was used for processing. For liver parenchyma, four ROIs measuring 20–40 mm^2 were placed on four different segments (right anterior, right posterior, left lateral, and left medial areas) on the level of the portal bifurcation avoiding large vessels and artifacts and averaged. ROI size and location was copied and pasted from pre- to postcontrast images, and the average SI was used for analysis. For SI measurements of HCCs, ROI were drawn as large as possible to encompass lesion size, and included viable and necrotic portions in case of treated lesions. The SI of reference lesions was measured twice in two adjacent slices and the averaged SI was used for analysis. A maximum number of seven HCCs per patient was recorded on the basis of the largest size.

The following quantitative parameters were calculated in viable HCCs for both GBCAs:

1. Enhancement ratio (ER) = [(SI post - SI pre)/SI pre] x100%, for liver parenchyma, hepatic vessels, and HCCs
2. Lesion-to-liver contrast ratio = (SI lesion - SI liver)/ (SI lesion + SI liver)
3. Wash-out-ratio for PVP and LVP = (SI PVP or LVP - SI AP2)/ SI AP2

Results are expressed as mean ± standard deviation.

Reference standard

Reference standard for HCC diagnosis was represented by histopathologic findings and consensus imaging evaluation by observers 3 and 4. Histopathologic diagnosis was obtained in 7/12 patients (surgical resection, $n=4$; and liver explant specimen, $n=3$). A lesion was diagnosed as HCC on CE MRI if it fulfilled the AASLD 2011 criteria (18) and for atypical enhancing nodules (AASLD negative) when lack of contrast retention on HBP on gadoxetic acid CE MRI with/ without hyperintensity on T2WI/DWI (when compared with surrounding liver parenchyma) was noted. The diagnosis of HCC for the remaining five patients was obtained by imaging follow-up (mean, 12 months; range, 5–24 months) showing response to subsequent TACE ($n=3$) or tumor progression ($n=2$).

Statistical analysis

Statistical analysis was performed using SPSS version 20. $P < 0.05$ indicated a statistically significant difference. No formal assessment of statistical power is provided in this exploratory study. A paired Wilcoxon test was used to compare the following parameters between gadopentetate dimeglumine and gadoxetic acid: enhancement ratios of liver, HCCs, and hepatic vessels; image quality; HCC lesion conspicuity; lesion-to-liver contrast ratio and wash-out ratio. To test the improvement in diagnostic performance of each method, the results provided by CE MRI using gadopentetate dimeglumine and gadoxetic acid were compared with the reference standard. Per-lesion sensitivity and PPV were computed in terms of concordance between the classification of patients and lesions as positive versus negative at reference standard and the classification of patients and lesions as test-positive versus test-negative for a given combination of reader and imaging features. Given the presence of treated lesions, complete necrotic HCCs were excluded from the detection/ conspicuity and quantitative lesion analysis.

Results

Reference standard

Twenty-one lesions were identified in 12 patients on MRI. Of these, 20/21 corresponded to HCCs (mean size, 2.6 cm; range, 1.0–5.0 cm). Histopathology was available in eight HCCs, and demonstrated the following: well differentiated (WD) ($n=1$), moderately differentiated (MD) ($n=4$), and poorly differentiated (PD) HCC ($n=1$), and two completely necrotic HCCs for which differentiation could not be established. One patient had one hemangioma measuring 15 mm and no HCC as noted on consensus imaging reference standard. The hemangioma showed wash-in and no wash-out on dynamic CE T1W imaging and hypointensity on HBP, and was found to be stable on follow-up imaging. The hemangioma was excluded from the quantitative lesion analysis. Eleven of 20 HCCs correspond to treatment-naïve and 9/20 to treated lesions (6/9 completely necrotic and 3/9 partially treated with persistent viable tumor). Of the 14 viable HCCs: 12/14 showed a hypervascular pattern of enhancement with

typical wash-in/wash-out, and 2/14 wash-in without wash-out on CE T1W imaging. On HBP, 11/14 HCCs were hypointense, 2/14 were hyperintense, and 1/14 had mixed signal intensity. Two HCCs showing hyperintense signal on HBP correspond to a WD and MD HCC on histopathology, and had typical wash-in/wash-out on dynamic postcontrast imaging.

MRI findings

Image quality and qualitative vessel enhancement. No significant difference was observed in image quality between both GBCAs for either observer (overall IQ score (max 16): 14 ± 2.4 vs. 13.9 ± 2.5, $P = 0.7$ for observer 1 and 15.0 ± 2.1 vs. 14.0 ± 2.3 for observer 2 for gadopentetate dimeglumine and gadoxetic acid, respectively). There was no significant difference in qualitative vascular enhancement between gadopentetate dimeglumine and gadoxetic acid, with the exception of higher scores for hepatic veins on gadopentetate dimeglumine-set (9.7 ± 1.6) vs. gadoxetic acid-set (7.3 ± 1.9, $P < 0.005$) for observer 2.

HCC detection. Treated necrotic HCCs ($n = 6$) were excluded from the detection and conspicuity analysis. Higher sensitivity were seen by observer 1 for a combined interpretation of dynamic CE T1W imaging and HBP on gadoxetic acid-set in comparison with gadopentetate dimeglumine-set (sensitivity increased from 85.7% to 92.8%), while no difference was noted for observer 2 (sensitivity of 78.5 for gadopentetate dimeglumine and gadoxetic acid-sets). The addition of HBP allowed observer 1 to correctly diagnose three atypical enhancing lesions as HCC on the gadoxetic acid-set. The two observers erroneously labeled the hemangioma as HCC with both contrast agents (false positive). PPV were similar for both GBCAs and for both observers (observer 1: 92.3 %, observer 2: 91.6%).

HCC lesion conspicuity. No significant differences in lesion conspicuity were observed between gadopentetate dimeglumine and gadoxetic acid CE T1W imaging dynamic phases, with the exception of higher lesion conspicuity score on AP1 with gadopentetate dimeglumine (3.9 ± 1.5) compared to gadoxetic acid-set (2.5 ± 1.7, $P < 0.007$) for observer 2. Conversely, lesion conspicuity was significantly higher on HBP compared to all CE T1W dynamic phase images (AP1, AP2, PVP, LVP) with gadopentetate dimeglumine for observer 2 ($P < 0.05$) and compared to AP1, AP2, and PVP phases with gadopentetate dimeglumine for observer 1 ($P < 0.03$). Higher lesion conspicuity on HBP (Fig. 1) in comparison with gadoxetic acid AP1, AP2, PVP, and LVP dynamic phases was also noted for observer 1 ($P < 0.01$). Lesion conspicuity was higher on HBP in comparison with gadoxetic acid AP1 and AP2 dynamic phases for observer 2 ($P < 0.01$). No significant differences for lesion conspicuity scores were found between gadoxetic acid HBP, PVP and LVP for observer 2.

Quantitative analysis of hepatic enhancement. Enhancement ratios were successfully measured for all 12 subjects. The results of mean ER in the liver parenchyma and

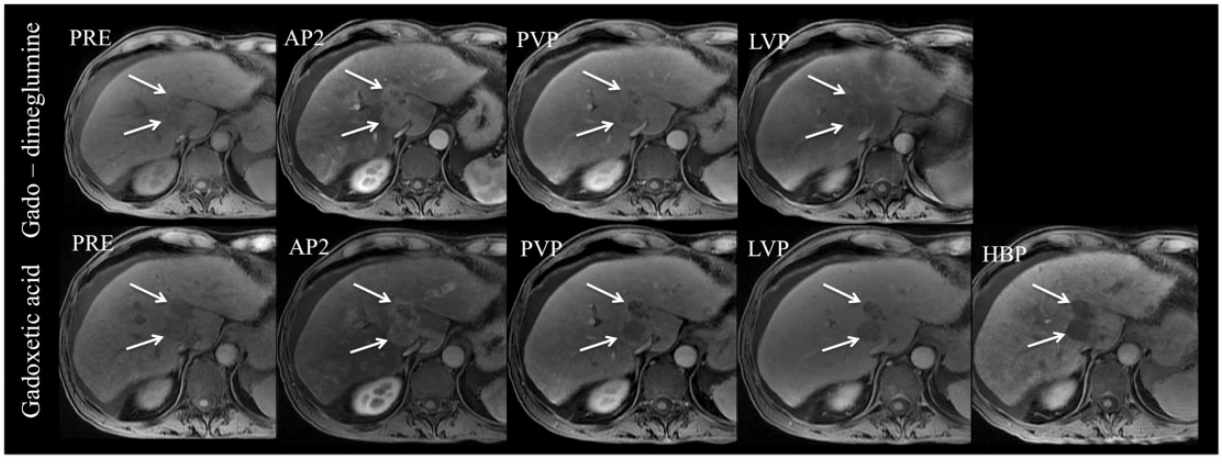

Fig. 1. A 58 year-old man with chronic hepatitis C related cirrhosis and multifocal HCC, evaluated with contrast-enhanced 3 T MRI using both gadopentetate dimeglumine and gadoxetic acid. Axial fat-suppressed 3D GRE T1W LAVA FLEX images through the liver before (PRE) and after injection of gadopentetate dimeglumine (top) and gadoxetic acid (bottom) at late arterial phase (AP2), portal venous phase (PVP), late venous phase (LVP), and hepatobiliary phase (HBP for gadoxetic acid). There are two adjacent hypervascular HCCs in the central liver, which demonstrate wash-in during AP2 and wash-out on PVP and LVP for both agents. HBP image obtained 20 min after gadoxetic acid injection demonstrates lack of contrast retention on the lesions, with higher lesion conspicuity.

Table 2. Enhancement ratios of liver parenchyma and vessels on CE T1W imaging obtained with gadopentetate dimeglumine and gadoxetic acid-sets on CE MRI at the dynamic phase.

	Phase	Gadopentetate dimeglumine	Gadoxetic acid	*P**
Liver parenchyma	AP1	4.2 ± 8.3	5.9 ± 9.2	0.44
	AP2	35.1 ± 14.5	24.7 ± 11.1	**0.026**
	PVP	64.0 ± 16.7	48.6 ± 7.7	**0.006**
	LVP	57.8 ± 16.6	45.7 ± 6.9	**0.013**
Abdominal aorta	AP1	158.8 ± 131.1	162.4 ± 65.5	0.59
	AP2	143.6 ± 95.0	121.7 ± 50.9	0.85
	PVP	137.7 ± 79.1	102.7 ± 45	**0.04**
	LVP	121.7 ± 86.1	82.6 ± 36.3	**0.008**
Portal vein	AP1	0.36 ± 16.3	9.14 ± 27.3	**0.002**
	AP2	77.3 ± 42.1	84.4 ± 48.9	0.75
	PVP	123.9 ± 50.3	127.0 ± 68.0	0.85
	LVP	113.0 ± 48.2	98.02 ± 53.0	0.62
Hepatic vein	AP1	32.8 ± 3.28	44.6 ± 74.7	0.95
	AP2	116.9 ± 53.7	96.3 ± 43.0	0.18
	PVP	111.1 ± 54.9	70.6 ± 40.0	**0.015**
	LVP	98.8 ± 46.3	61.9 ± 38.4	**0.008**

Data are expressed as mean ± SD.
*Paired Wilcoxon test (significant *P* values are bold).
AP1, early arterial phase; AP2, late arterial phase; LVP, late venous phase; PVP, portal venous phase.

Table 3. Enhancement ratios (ER), lesion-to-liver contrast ratios, and wash-out ratios of 14 viable hepatocarcinoma (HCCs) on CE T1W imaging obtained with gadopentetate dimeglumine and gadoxetic acid on dynamic phases and HBP.

	Phase	Gadopentetate dimeglumine	Gadoxetic acid	*P**
Enhancement ratio	AP1	31.7 ± 28.5	16.5 ± 29.6	0.1
	AP2	69.7 ± 25.8	62.9 ± 42.7	0.14
	PVP	71.0 ± 18.4	53.3 ± 28.9	**0.01**
	LVP	58.6 ± 14.6	48.3 ± 27.3	**0.01**
	HBP	–	27.4 ± 34.6	–
Lesion-to-liver contrast ratio	AP1	0.02 ± 0.1	–0.09 ± 0.1	**0.01**
	AP2	–0.03 ± 0.1	0.03 ± 0.1	0.97
	PVP	–0.10 ± 0.1	–0.14 ± 0.1	**0.009**
	LVP	–0.11 ± 0.1	–0.14 ± 0.1	**0.01**
	HBP	–	–0.18 ± 0.1	–
Wash-out ratio	PVP	1.5 ± 8.1	–3.6 ± 9.8	0.15
	LVP	–5.3 ± 10.8	–6.2 ± 13.3	0.77

Data are expressed as mean ± SD.
Liver-to-lesion contrast ratios were significantly higher for HBP compared to all dynamic phases (AP1, AP2, PVP, LVP) for gadopentetate dimeglumine-set and compared to AP1–AP2 for gadoxetic acid-set ($P < 0.001$).
*Paired Wilcoxon test (significant *P* values are bold).
AP1, early arterial phase; AP2, late arterial phase; HBP, hepatobiliary phase; LVP, late venous phase; PVP, portal venous phase.

major hepatic vessels (aorta and portal vein) on CE T1W imaging obtained with gadopentetate dimeglumine-set and gadoxetic acid-set are summarized in Table 2. ER of normal liver parenchyma increased over time for both contrast agents. Liver ERs were significantly higher in AP2, PVP, and LVP with gadopentetate dimeglumine-set ($P < 0.01$). Regarding hepatic vessel enhancement, the mean ER of aorta and hepatic vein were significantly lower on PVP and LVP phases with gadoxetic acid-set than with gadopentetate dimeglumine-set ($P < 0.01$).

ER values were obtained in 14 viable HCCs (Table 3). The ERs of HCC at PVP and LVP were significant lower with gadoxetic acid-set than with gadopentetate dimeglumine-set ($P < 0.01$). No significant differences were found for ER of HCCs at AP1 or AP2 between both contrast agents (Fig. 2). Lesion-to-liver contrast ratios were significantly higher in the gadoxetic acid-set in comparison than with gadopentetate dimeglumine-set for all CE T1W dynamic phases ($P < 0.05$), with the exception of AP2. In addition, lesion-to-liver contrast ratios were significantly higher for HBP compared to all CE T1W dynamic phases (AP1, AP2, PVP, LVP) for gadopentetate dimeglumine and for gadoxetic acid-set ($P < 0.05$). No significant difference in wash-out ratio for HCC in PVP or LVP was identified between gadopentetate dimeglumine-set and gadoxetic acid-set. Fig. 3 shows the typical dynamic enhancement pattern of HCC on CE T1W MRI with gadopentetate dimeglumine and gadoxetic acid.

Discussion

Gadopentetate dimeglumine and more recently gadoxetic acid are GBCAs with an established role in liver lesion detection and characterization (20–22), including HCC detection. In our study we prospectively compared 3D CE T1W images obtained at 3 T using both gadopentetate dimeglumine and gadoxetic acid in patients with chronic liver disease and HCC. Extracellular GBCAs are still the most widely used MR contrast agents for HCC evaluation, and therefore the differences between these contrast agents and gadoxetic acid must be determined.

Our quantitative analysis demonstrated lower liver enhancement with gadoxetic acid compared to gadopentetate dimeglumine for all CE T1W dynamic phases. This is expected given the lower contrast dose used for gadoxetic acid (0.03 mmol/kg vs. 0.1 mmol/kg), and has also been described in previous reports (4,5,23,24). However, no differences in image quality were observed between the two GBCAs in our initial results.

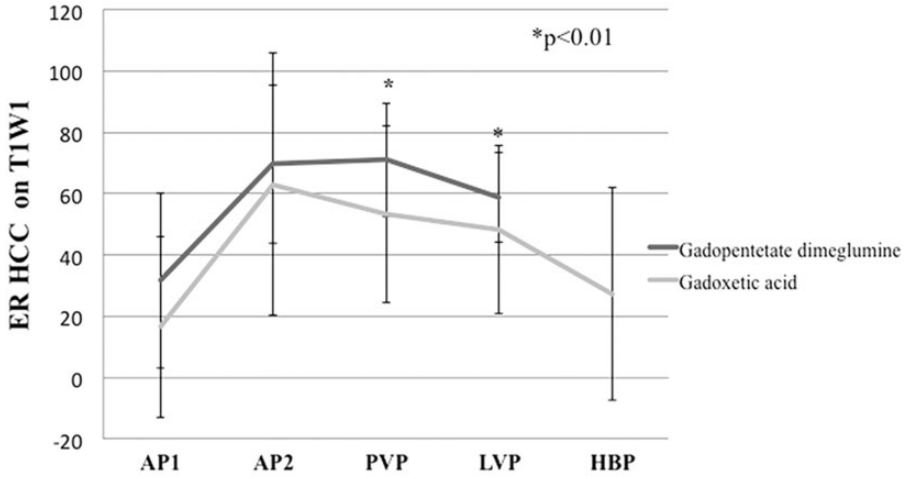

Fig. 2. Plots of ER (enhancement ratios) vs. time of viable HCCs on T1W imaging after injection of gadopentetate dimeglumine and gadoxetic acid. HCC tumors show progressive enhancement with the use of both contrast agents during early (AP1) and late (AP2) arterial phases, with decrease of ER over time on portal venous (PVP) and late venous (LVP) phases and hepatobiliary phase (HBP) with gadoxetic acid. Lower ER was seen on HBP in comparison with PVP and LVP in HCC for both contrast agents. Mean ERs of gadopentetate dimeglumine (grey curve) are higher than those of gadoxetic acid (white curve), with a significant difference observed for PVP and LVP phases ($P < 0.01$).

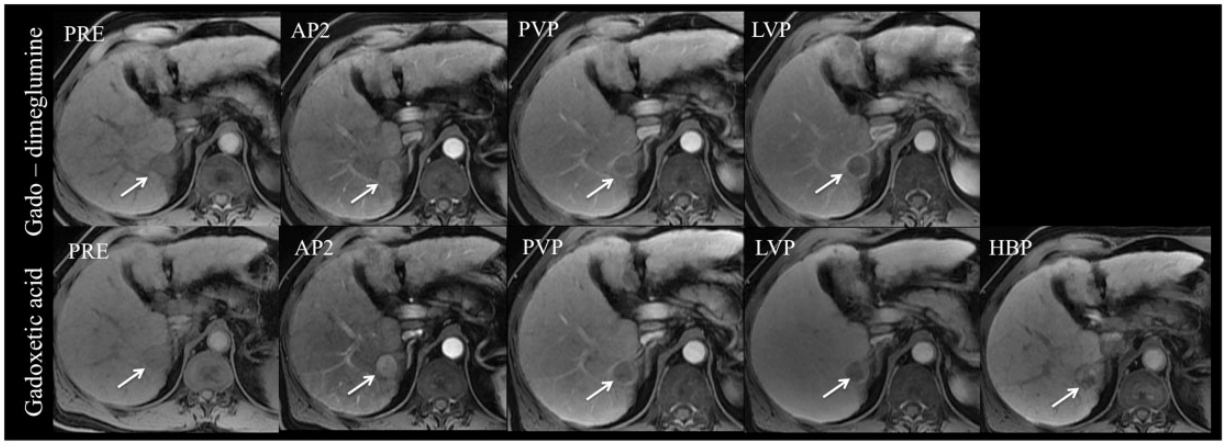

Fig. 3. A 60 year-old man with chronic hepatitis C cirrhosis and moderately differentiated HCC evaluated with contrast-enhanced 3 T MRI after the use of gadopentetate dimeglumine and gadoxetic acid. Axial fat-suppressed 3D GRE T1W LAVA FLEX images through the liver before (PRE) and after injection of gadopentetate dimeglumine (top) and gadoxetic acid (bottom) at late arterial (AP2) phases, portal venous phase (PVP), late venous phase (LVP), and hepatobiliary phase (HBP for gadoxetic acid). Both contrast agents demonstrate similar pattern and degree of enhancement of the liver and aorta/hepatic vessels during AP and PVP. There is a 2 cm hypervascular HCC in the right hepatic lobe (arrow), which demonstrates wash-in during AP2 phases for both contrast agents. The lesion shows wash-out on PVP and LVP. HBP image demonstrates mixed signal intensity in the lesion with some degree of contrast retention.

We found higher sensitivity for a combined interpretation of dynamic CE T1W imaging and HBP on gadoxetic acid-set versus gadopentetate dimeglumine-set for one observer (sensitivity increased from 85.7% to 92.8%), while no difference was noted for observer 2 (sensitivity of 78.5 for both GBCAs). Improved lesion conspicuity was found for both observers by including HBP images with gadoxetic acid. In our study, most viable HCCs ($10/14 = 71.4\%$) demonstrated arterial enhancement with wash-out on venous phase fulfilling AASLD criteria for HCC diagnosis. However, three atypical enhancing hypovascular nodules were correctly characterized as HCC by one observer with the addition of HBP images. When extracellular GBCAs are

used, small HCCs may appear isointense on delayed imaging, limiting HCC detection. The use of gadoxetic acid with HPB images has been shown to improve the diagnosis of small HCC and assist in surgical planning (3,12,25).

Higher HCC enhancement ratios were found with the use of gadopentetate dimeglumine in comparison with gadoxetic acid, with a significant difference observed for PVP and LVP phases ($P < 0.01$). However, no significant differences were found on early and late arterial phases (AP1 and AP2) between the two contrast agents, which confirm that delineation of HCC arterial hyper vascularization by gadoxetic acid is comparable to that of extracellular gadolinium agents, despite the lower injected dose, which is counterbalanced by higher T1 relaxivity (3.7 L $mmol^{-1}$ s^{-1} for gadopentetate dimeglumine versus 6.2 L $mmol^{-1}$ s^{-1} for gadoxetic acid measured in human blood at 3 T) (26). Lesion-to liver contrast ratios were significantly higher for HBP compared to all CE T1W dynamic phases for gadopentetate dimeglumine-set and for gadoxetic acid-set. In addition, higher lesion conspicuity score was found on HBP compared to early and late arterial phases on both gadopentetate dimeglumine and gadoxetic acid-sets for both observers. These findings are consistent with previous reports showing improved tumor conspicuity using gadoxetic acid in comparison with gadopentetate dimeglumine MRI due to increased contrast between liver parenchyma and focal lesions during HBP (4,15,27).

There are several limitations to this study. First, the sample size was small, as this was an initial experience. Therefore, these results should be verified in a larger prospective study. Second, we did not obtain histopathologic verification in all tumors and histopathologic reference standard for HCC was generated on the basis of imaging report; with only 3/12 patients who underwent liver transplantation with knowledge of exact total number of HCC lesions; therefore, the possibility of missed HCCs is not completely excluded. Futures research studies using MRI–liver explant correlation should be performed to overcome this limitation. Although, HCCs non-verified histologically were diagnosed using validated imaging appearance, which is considered sufficient for clinical diagnosis of HCC (18). Third, selection bias existed because we included only patients who were suspected of having HCC based on previous imaging studies, without negative or control cases provided. Thus, observers were aware before of the image interpretation that all patients were likely to have HCC lesions. Thus, sensitivity values may be overestimated.

In conclusion, the results from our prospective crossover study suggest that gadoxetic acid-set including HBP was superior to gadopentetate dimeglumine-set in terms of HCC detection for one observer, with improved lesion conspicuity and liver-to-lesion contrast using HBP compared to CE T1W dynamic phases of enhancement for both GBCAs. Equivalent image quality was found between both gadolinium contrast agents (GBCAs).

Conflict of interest

BT is a consultant for Bayer Healthcare.

Ethical approval

This project is approved by the Institutional Review Board of Mount Sinai Hospital and Medical Center.

Funding

Bayer Healthcare.

References

1. El-Serag HB. Epidemiology of hepatocellular carcinoma in USA. Hepatol Res 2007;37(Suppl. 2): S88–S94.
2. Burrel M, Llovet JM, Ayuso C, et al. MRI angiography is superior to helical CT for detection of HCC prior to liver transplantation: an explant correlation. Hepatology 2003; 38:1034–1042.
3. Park MS, Kim S, Patel J, et al. Hepatocellular carcinoma: detection with diffusion-weighted versus contrast-enhanced magnetic resonance imaging in pretransplant patients. Hepatology 2012;56:140–148.
4. Vogl TJ, Kummel S, Hammerstingl R, et al. Liver tumors: comparison of MR imaging with Gd-EOB-DTPA and Gd-DTPA. Radiology 1996;200:59–67.
5. Tamada T, Ito K, Sone T, et al. Dynamic contrast-enhanced magnetic resonance imaging of abdominal solid organ and major vessel: comparison of enhancement effect between Gd-EOB-DTPA and Gd-DTPA. J Magn Reson Imaging 2009;29:636–640.
6. Ringe KI, Husarik DB, Sirlin CB, et al. Gadoxetate disodium-enhanced MRI of the liver: part 1, protocol optimization and lesion appearance in the noncirrhotic liver. Am J Roentgenol 2010;195:13–28.
7. Cruite I, Schroeder M, Merkle EM, et al. Gadoxetate disodium-enhanced MRI of the liver: part 2, protocol optimization and lesion appearance in the cirrhotic liver. Am J Roentgenol 2010;195:29–41.
8. Ichikawa T, Saito K, Yoshioka N, et al. Detection and characterization of focal liver lesions: a Japanese phase III, multicenter comparison between gadoxetic acid disodium-enhanced magnetic resonance imaging and contrast-enhanced computed tomography predominantly in patients with hepatocellular carcinoma and chronic liver disease. Invest Radiol 2010;45:133–141.
9. Halavaara J, Breuer J, Ayuso C, et al. Liver tumor characterization: comparison between liver-specific gadoxetic acid disodium-enhanced MRI and biphasic CT–a multicenter trial. J Comput Assist Tomogr 2006;30:345–354.

10. Raman SS, Leary C, Bluemke DA, et al. Improved characterization of focal liver lesions with liver-specific gadoxetic acid disodium-enhanced magnetic resonance imaging: a multicenter phase 3 clinical trial. J Comput Assist Tomogr 2010;34:163–172.
11. Hamm B, Staks T, Muhler A, et al. Phase I clinical evaluation of Gd-EOB-DTPA as a hepatobiliary MR contrast agent: safety, pharmacokinetics, and MR imaging. Radiology 1995;195:785–792.
12. Ahn SS, Kim MJ, Lim JS, et al. Added value of gadoxetic acid-enhanced hepatobiliary phase MR imaging in the diagnosis of hepatocellular carcinoma. Radiology 2010; 255:459–466.
13. Sano K, Ichikawa T, Motosugi U, et al. Imaging study of early hepatocellular carcinoma: usefulness of gadoxetic acid-enhanced MR imaging. Radiology 2011;261: 834–844.
14. Park MJ, Kim YK, Lee MW, et al. Small hepatocellular carcinomas: improved sensitivity by combining gadoxetic acid-enhanced and diffusion-weighted MR imaging patterns. Radiology 2012;264:761–770.
15. Clement O, Muhler A, Vexler VS, et al. Comparison of Gd-EOB-DTPA and Gd-DTPA for contrast-enhanced MR imaging of liver tumors. J Magn Reson Imaging 1993;3:71–77.
16. Park G, Kim YK, Kim CS, et al. Diagnostic efficacy of gadoxetic acid-enhanced MRI in the detection of hepatocellular carcinomas: comparison with gadopentetate dimeglumine. Br J Radiol 2010;83:1010–1016.
17. Park Y, Kim SH, Kim SH, et al. Gadoxetic acid (Gd-EOB-DTPA)-enhanced MRI versus gadobenate dimeglumine (Gd-BOPTA)-enhanced MRI for preoperatively detecting hepatocellular carcinoma: an initial experience. Korean J Radiol 2010;11:433–440.
18. Bruix J, Sherman M. American Association for the Study of Liver D. Management of hepatocellular carcinoma: an update. Hepatology 2011;53:1020–1022.
19. Kim S, Mannelli L, Hajdu CH, et al. Hepatocellular carcinoma: assessment of response to transarterial chemoembolization with image subtraction. J Magn Reson Imaging 2010;31:348–355.
20. Balci NC, Semelka RC. Contrast agents for MR imaging of the liver. Radiol Clin North Am 2005;43:887–898.
21. Lebedis C, Luna A, Soto JA. Use of magnetic resonance imaging contrast agents in the liver and biliary tract. MRI Clin North Am 2012;20:715–737.
22. Seale MK, Catalano OA, Saini S, et al. Hepatobiliary-specific MR contrast agents: role in imaging the liver and biliary tree. Radiographics 2009;29:1725–1748.
23. Kuhn JP, Hegenscheid K, Siegmund W, et al. Normal dynamic MRI enhancement patterns of the upper abdominal organs: gadoxetic acid compared with gadobutrol. Am J Roentgenol 2009;193:1318–1823.
24. Fujinaga Y, Ohya A, Matsushita T, et al. Effect of hepatobiliary uptake of Gd-EOB-DTPA on the hepatic venous phase of dynamic magnetic resonance imaging on a 3.0-T apparatus: comparison between Gd-EOB-DTPA and Gd-DTPA. Jpn J Radiol 2011;29:695–700.
25. Bashir MR, Gupta RT, Davenport MS, et al. Hepatocellular carcinoma in a North American population: Does hepatobiliary MR imaging with Gd-EOB-DTPA improve sensitivity and confidence for diagnosis? J Magn Reson Imaging 2013;37:398–406.
26. Rohrer M, Bauer H, Mintorovitch J, et al. Comparison of magnetic properties of MRI contrast media solutions at different magnetic field strengths. Invest Radiol 2005; 40:715–724.
27. Korkusuz H, Knau LL, Kromen W, et al. Different signal intensity at Gd-EOB-DTPA compared with Gd-DTPA-enhanced MRI in hepatocellular carcinoma transgenic mouse model in delayed phase hepatobiliary imaging. J Magn Reson Imaging 2012;35:1397–1402.